

Characteristics of highly excited diatomic rovibrational spectra and slow atomic collisions

Bo Gao

Department of Physics and Astronomy, University of Toledo, Toledo, Ohio 43606

(November 11, 2018)

Abstract

We show that the highly excited rovibrational spectra of a diatomic molecule and the closely related slow atomic collision processes contain more systematics and require less parameters to characterize than the Rydberg spectrum of an atom. In the case of a single channel, for example, we show that a *single* short-range parameter gives a complete description of slow collisions for practically all angular momenta, and covers an energy range of hundreds of millikelvins. The *same* parameter also describes the highly excited rovibrational spectra in the threshold region, including states of different angular momenta. Sample applications and predictions of the theory are discussed, including comparisons with experiment.

PACS number(s): 34.10.+x,33.20.Vq,32.80.Pj

This paper examines the properties of a two-atom system in a small energy region around a dissociation threshold, with the region above corresponding to slow atomic collisions, and the region below containing the highly excited rovibrational states of the corresponding diatomic molecule. We discuss a type of systematics that relate states of different relative angular momenta, thus greatly simplifying our understanding of such systems. Comparison of the theory with existing experimental data [1] also provides the first verification of the breakdown of the large-quantum-number formulation of the correspondence principle [2–4].

With recent developments such as the analytic solutions of the Schrödinger equation for $1/r^6$ and $1/r^3$ potentials [5,6,4], our understanding of two-atom systems is already conceptually comparable to the quantum defect theory (QDT) of atomic Rydberg spectra [7]. Namely, the slow atomic scattering and the rovibrational spectrum of a particular angular momentum can be understood in terms of the long range solutions and a parameter that is a slowly varying function of energy in the threshold region [5,8,9,6,4]. In this work, we show that a two-atom system possesses an even greater degree of systematics in the following sense. Unlike the QDT for atomic Rydberg spectra in which different angular momentum states have different quantum defects with no general relationships among them, a single parameter is sufficient to characterize slow atomic collisions for practically all angular momenta. The same parameter also characterizes the rovibrational spectra in the threshold region, including states of different angular momenta. In other words, in addition to the relationship between the bound spectrum and scattering, as expected from traditional QDT formulations, a two-atom system has also the unique property that scattering of different angular momenta are related, and so are the bound spectra of different angular momenta. While a similar idea can be implemented in a numerical fashion [1], it becomes a much more powerful tool in the present formulation.

The origin of this systematics is not difficult to understand and is due to a combination of the following three properties of a typical molecular system. (a) Atoms are strongly repulsive at short distances. (b) Atoms are heavy compared to electrons. (c) The atom-atom interaction at large distances behaves as $1/r^n$ with $n > 2$.

The combination of the first two properties gives rise to the well-known separation of tightly bound rovibrational states into the product of two parts $\psi_v\psi_r$, in which the vibrational wave function ψ_v is, to the lowest order, independent of rotational quantum numbers. For rovibrational states that are highly excited, the same properties ensure that the radial wave function, up to a normalization constant, remain nearly independent of the angular momentum until a distance is reached where the rotational energy term becomes comparable to the electronic and other energy terms. This characteristic is uniquely molecular and does not apply to the electronic wave functions of an atom, for which the rotational term dominates the behavior at sufficiently small r .

The implication of the third property can be understood from qualitative behaviors of the effective potential $-C_n/r^n + \hbar^2 l(l+1)/(2\mu r^2)$, in which the first term represents the long range interaction and the second term represents the centrifugal barrier. For $n > 2$ and $l \neq 0$, this potential has a maximum and crosses zero at $r_x = [l(l+1)]^{-1/(n-2)} \beta_n$, where β_n is a length scale associated with the $-C_n/r^n$ interaction as defined by

$$\beta_n \equiv (2\mu C_n/\hbar^2)^{1/(n-2)}. \quad (1)$$

From a physical point of view, r_x specifies the location at which the rotational potential is equal to the long range interaction. For an l that is not too large, r_x is of the order of β_n . Since n is greater than two, for distances that are smaller than r_x , the long range interaction quickly dominates, and correspondingly, the importance of the angular momentum quickly diminishes. Mathematically speaking, this means that for a potential that goes to zero faster than $1/r^2$ at large distances, a pair of linearly independent solutions exist, which, at relatively small distances, are not only independent of energy, but also independent of angular momentum.

The combination of these characteristics leads to the following important conclusion. With proper choice of long range solutions, a quantum defect theory for molecular rovibrational states and slow atomic collisions can be formulated in which the short-range parameters are not only nearly independent of energy, but also nearly independent of the relative

angular momentum. This conclusion is very general and powerful. Its formulation and application are illustrated here for a single channel problem with a van der Waals asymptotic interaction. The formulation for attractive $1/r^3$ interaction and multichannel generalizations will be presented elsewhere [10].

For a single channel with an asymptotic van der Waals interaction ($-C_6/r^6$), the proper pair of long range solutions are ones with the behavior

$$f_{\ell}^c \xrightarrow{r \ll \beta_6} (2/\pi)^{1/2} (r/\beta_6) r^{1/2} \cos \left(\frac{1}{2} (r/\beta_6)^{-2} - \frac{\pi}{4} \right), \quad (2)$$

$$g_{\ell}^c \xrightarrow{r \ll \beta_6} -(2/\pi)^{1/2} (r/\beta_6) r^{1/2} \sin \left(\frac{1}{2} (r/\beta_6)^{-2} - \frac{\pi}{4} \right), \quad (3)$$

for both positive and negative energies. This pair, which has not only energy-independent, but also angular-momentum-independent behavior at small distances, is related to the f^0 and g^0 pair defined in [5] by a linear transformation. The fact that such a pair exist is a result of the exponent n that characterizes the long range interaction, $-C_n/r^n$, being greater than 2.

With this choice of long range solutions, the single channel quantum defect theory is still formally the same as discussed previously [8,6,4]. In particular, the bound spectrum of any potential with the behavior of $V(r) \rightarrow -C_6/r^6$ at large distances is still given rigorously by the crossing points between a χ function and a short-range K matrix [8,4]:

$$\chi_l^c(\epsilon_s) = K^c(\epsilon, l). \quad (4)$$

Here ϵ_s is a scaled bound state energy defined by

$$\epsilon_s = \frac{1}{16} \frac{\epsilon}{(\hbar^2/2\mu)(1/\beta_6)^2}. \quad (5)$$

The χ^c function, corresponding to the choice of long range solutions as specified by Eqs. (2) and (3), is given by

$$\chi_l^c(\epsilon_s) = \frac{(Y_{\ell l}/X_{\ell l}) + \tan(\pi\nu/2)(1 + M_{\ell l})/(1 - M_{\ell l})}{1 - (Y_{\ell l}/X_{\ell l}) \tan(\pi\nu/2)(1 + M_{\ell l})/(1 - M_{\ell l})}, \quad (6)$$

in which $M_{\ell l} = G_{\ell l}(-\nu)/G_{\ell l}(\nu)$, with ν and $G_{\ell l}$ being defined in [5]. Plots of χ_l^c functions for different l are shown in Figure 1. K^c is the short range K matrix that results from the matching of the short range solution and the long range solution. It is given specifically by

$$K^c(\epsilon, l) = \left(\frac{f_{\ell l}^c}{g_{\ell l}^c} \right) \frac{(f_{\ell l}^{c'}/f_{\ell l}^c) - (u_{\ell l}'/u_{\ell l})}{(g_{\ell l}^{c'}/g_{\ell l}^c) - (u_{\ell l}'/u_{\ell l})}, \quad (7)$$

evaluated at any radius beyond r_0 at which the potential has become well represented by $-C_n/r^n$.

Above the threshold, the scattering K matrix is given by a similar expression as derived previously [8,6,4]:

$$K_l \equiv \tan \delta_l = (K^c Z_{gg}^c - Z_{fg}^c)(Z_{ff}^c - K^c Z_{gf}^c)^{-1}, \quad (8)$$

with the Z^c matrix being related to the Z matrix defined in [5] by a linear transformation.

The key difference between the present formulation and the previous one is the following. With the choice of long range solution pair as specified by Eqs. (2) and (3), and the property of the wave function discussed earlier, the parameter K^c is, under the condition of $\beta_n \gg r_0$ [8,6,4], not only independent of energy, but also independent of angular momentum l in the threshold region [see Eq. (7)]. In other words, a single parameter, K^c , can describe scattering and bound states of different angular momenta.

The determination of the parameter K^c is, in principle, straightforward theoretically. It can be done, for example, by solving the radial equation at a small energy (include zero energy) and matching it to the proper long range solution. However, since our present knowledge about both the short range interaction and the C_n coefficients is still not sufficiently accurate for many systems, we focus here on the direct experimental determination of both the K^c parameter and the C_n coefficient. In particular, we show that if the C_n coefficient that characterizes the dominant long range interaction is known accurately, the parameter K^c can be obtained from the measurement of a single binding energy (similar to the determination of K_l^0 discussed previously [8]). If binding energies of more than one state are known, in addition to the prediction of the parameter K^c , an accurate determination of C_n can also be made, especially when the two states are closely spaced in energy.

In Table I, the first column presents the experimental results [1] for states of $^{85}\text{Rb}_2$ characterized by quantum numbers $F_1 = 3$, $F_2 = 3$, $F = 6$, $l = 2$, and $T = 8$ [11,12]. The results in the column labeled by Theory II represents a simple calculation making use of only a single experimental energy. In this calculation, the energy of the level labeled by $v_{max} - v = 1$ in Table I is first scaled according to Eqs. (5) and (1) with $\mu = 77392.368$ a.u. and a value of $C_6 = 4426$ a.u. from the theoretical calculation of Marinescu *et al.* [13]. The parameter K^c is determined by evaluating the $\chi_{l=2}^c$ function at this scaled energy [8], which yields a value of $K^c = 0.2841$. The crossing points of this constant with $\chi_{l=2}^c(\epsilon_s)$ give the predictions of the other energy levels listed in this column (see Fig. 1). Note that this simple calculation already yields excellent agreement with experiment and compares very favorably with a much more complex numerical calculation [1] listed under Theory I in Table I. This excellent agreement shows that the parameter K^c is indeed, to a very good approximation, a constant in the energy range covered by the experiment (~ 10 GHz). This is further confirmed by the fact that enforcing K^c to be constant leads to an even better agreement, a procedure that demonstrates a new method for the experimental determination of the leading C_n coefficient from a minimum of only two binding energy measurements.

Keeping in mind that the C_6 value used in the first calculation is not necessarily the true C_6 , it is allowed to vary in the following calculation. With more than one experimental binding energy available, we vary C_6 in such a way that the two χ^c 's evaluated at the two different scaled energies (they may also correspond to different l .) are the same, in other words, we force the parameter K^c to be a constant. The refined C_6 is then given by the root of the following equation

$$\chi_l^c(\epsilon_{s1}) - \chi_{l'}^c(\epsilon_{s2}) = 0, \quad (9)$$

where ϵ_{s1} and ϵ_{s2} are two experimental energies scaled according to Eqs. (5) and (1) for van der Waals interactions. The reduced masses are known with great precision from atomic masses so that the only unknown on the left hand side is the C_6 coefficient. This procedure, when applied to the two d states labeled in Table I by $v_{max} - v = 1$ and 2, respectively, leads to

a revised $C_6 = 4533$ a.u., which is in good agreement with $C_6 = 4550 \pm 100$ a.u., determined by Boesten *et al.* [14]. This C_6 value refines the energy scaling and leads to a revised value of $K^c = 0.3106$. The column in Table I labeled as Theory III gives the result of energy levels predicted using this set of revised parameters, and an even better agreement with experiment is achieved. This procedure demonstrates a new method for the determination of the C_n coefficient from two or more values of experimental binding energies. It requires no knowledge of the short range interactions, nor does it require numerical solutions of the Schrödinger equation. The closer in energy those two states are, the better this method works.

As stated earlier, the parameter K^c describes not only the rovibrational states of a particular relative angular momentum, but also the other angular momentum states in the threshold region (see Fig. 1). Table II gives the predictions of the bound spectra of $^{85}\text{Rb}_2$ characterized by quantum numbers $F_1 = 3, F_2 = 3, F = 6, l, T = F + l$, with $l = 0, 2, 4, 6$, respectively [11]. They are predicted using parameters $C_6 = 4533$ a.u. and $K^c = 0.3106$.

The fact that K^c is nearly a constant in the threshold region has also the following important implications. (a) It provides an experimental verification of the breakdown of the large-quantum-number formulation of the correspondence principle, as a semiclassical theory would have predicted different results for, e.g., the spacing between scaled energies [4]. (b) Since 1 GHz corresponds to 47.99 mK, the fact that K^c is independent of energy over a range of 10 GHz below the threshold implies that the same constant K^c can describe collisions over hundreds of millikelvins above the threshold (for all l 's that are not too large). (Similar conclusion can also be derived for Li [8,10]). All the energy and angular momentum dependences in this energy range, including shape resonances, are determined by the dominant long range interaction, in combination with the centrifugal barrier. And they are described analytically by the solutions for the long range potentials [5,6,4]. This result, along with the fact that for small energies, the scattering for large angular momentum is nearly independent of the value of K^c and is determined entirely by the long range interaction, means also that the same parameter describes slow collisions for practically all

angular momenta. As one implication, a single short-range parameter (a few parameters in the case of multichannels [10]) describes not only the ultracold region of energies, but also the region of evaporative cooling and the region of laser cooling. In contrast, in the traditional effective range expansion, a single parameter, the scattering length, gives little more than the cross section at zero energy. Figure 2 shows the partial scattering cross sections for s , d , and g waves predicted by the same short range parameter $K^c = 0.3106$ for two spin-polarized ^{85}Rb atoms in state $F_1 = 3$, $M_{F_1} = 3$, $F_2 = 3$, and $M_{F_2} = 3$. Only a small energy range is shown here to make for easy identification of the narrow g wave shape resonance, observed previously by Boesten *et al.* [14]. More data on the scattering cross sections, including those for larger angular momenta and over a greater energy range, and the summation formulae for summing over all angular momentum states will be presented elsewhere [10]. (c) Since the hyperfine splitting is typically of the order of 1 GHz, it means that the frame-transformation method for atom-atom scattering [12], when properly formulated with K^c (or the K_l^0 [8,6]) being the short range parameter [10], should work well in a multichannel formulation that includes hyperfine structures [12,9].

In conclusion, a theory of slow atomic collisions and molecular rovibrational states has been formulated that takes full advantage of the intrinsic characteristics of a typical molecular system. This formulation establishes a simple relationship between states of different relative angular momenta and greatly reduces the number of parameters required to describe slow atomic collisions and highly excited molecular rovibrational spectra. Multichannel generalizations do not change the key concepts in any substantial way, and the theory can also be implemented in exact numerical calculations. As far as parameterization is concerned, the theory can be further extended to an even greater range of energies by, e.g., taking into account the energy and angular momentum dependences induced by the correction terms to the dominant long range interaction [15]. Finally, the good agreement between the theory and experiment provides the first experimental confirmation of the breakdown of the large-quantum-number formulation of the correspondence principle [2-4].

I thank Anthony F. Starace and Tom Kvale for careful reading of the manuscript and

for helpful discussions. This work is supported by National Science Foundation under Grant No. PHY-9970791.

REFERENCES

- [1] C. C. Tsai *et al.*, Phys. Rev. Lett. **79**, 1245 (1997).
- [2] J. Trost *et al.*, J. Phys. B **31**, 361 (1998).
- [3] C. Boisseau *et al.*, Europhys. Lett. **41**, 349 (1998).
- [4] B. Gao, Phys. Rev. Lett. **83**, 4225 (1999).
- [5] B. Gao, Phys. Rev. A **58**, 1728 (1998);
- [6] B. Gao, Phys. Rev. A **59**, 2778 (1999).
- [7] M. J. Seaton, Rep. Prog. Phys. **46**, 167 (1983); U. Fano and A.R.P. Rau, *Atomic Collisions and Spectra* (Academic Press, Orlando, 1986); C. H. Greene and L. Kim, Phys. Rev. A **38**, 5953 (1988); F. Mies, Mol. Phys. **14**, 953 (1980).
- [8] B. Gao, Phys. Rev. A **58**, 4222 (1998).
- [9] J. P. Burke, Jr. *et al.*, Phys. Rev. Lett. **80**, 2097 (1998).
- [10] B. Gao, unpublished.
- [11] Here T refers to the total angular momentum of the two-atom system. See [12].
- [12] B. Gao, Phys. Rev. A **54**, 2022 (1996).
- [13] M. Marinescu, H. R. Sadeghpour, and A. Dalgarno, Phys. Rev. A, **49**, 982 (1994).
- [14] H.M.J.M. Boesten *et al.*, Phys. Rev. Lett. **77**, 5194 (1996).
- [15] Those terms lead to only small corrections around the threshold as their effects come in at $(\beta_8/\beta_6)^6$.

FIGURES

FIG. 1. The χ_l^c functions for an attractive $1/r^6$ interaction plotted vs $(\epsilon_s)^{1/3}$. Solid line: $l = 0$; Dash line: $l = 1$; Dash-dotted line: $l = 2$ dotted line: $l = 3$. The bound spectra of any potential with $V(r) \rightarrow -C_6/r^6$ at large distances is given by the crossing points of this *same* set of functions with a set of short range parameters $K^c(\epsilon, l)$. For systems that satisfy $\beta_6 \gg r_0$, $K^c(\epsilon, l)$ is approximately an *l-independent* constant in the threshold region, and the bound spectra of different angular momenta are given by the crossing points of χ_l^c functions with a single horizontal line representing $K^c = \text{const}$. The solid horizontal line in this figure corresponds to $K^c = 0.3106$. Its crossing points with χ_l^c , along with the energy scaling factor determined by $C_6 = 4533$ a.u. and $\mu = 77392.368$ a.u., give the binding energies of $^{85}\text{Rb}_2$ presented in the last columns of Table I and Table II.

FIG. 2. Partial scattering cross sections for a pair of spin-polarized ^{85}Rb atoms in state $F_1 = 3$, $M_{F1} = 3$, $F_2 = 3$, and $M_{F2} = 3$. $\beta_6 = 162.7$ a.u. is determined with $\mu = 77392.368$ a.u. and $C_6 = 4533$.

TABLES

TABLE I. Comparison of energies, in GHz, of the last four bound states of $^{85}\text{Rb}_2$ characterized by quantum numbers $F_1 = 3, F_2 = 3, F = 6, l = 2, T = 8$.

$v_{max} - v$	Experiment ^a	Theory I ^b	Theory II ^c	Theory III ^d
0	-0.16 ± 0.03	-0.15	-0.1513	-0.1539
1	-1.52 ± 0.03	-1.50	-1.520	-1.520
2	-5.20 ± 0.03	-5.16	-5.222	-5.200
3	-12.22 ± 0.06	-12.21	-12.37	-12.30

^aFrom [1].

^bFrom [1].

^c $C_6 = 4426$ a.u. and $K^c = 0.2841$.

^d $C_6 = 4533$ a.u. and $K^c = 0.3106$.

TABLE II. Bound state energies (in GHz) of $^{85}\text{Rb}_2$ with quantum numbers $F_1 = 3, F_2 = 3, F = 6, l, T = F + l$ with $l = 0, 2, 4, 6$, respectively. They are predicted using $C_6 = 4533$ a.u. and $K^c = 0.3106$.

$l = 0$	$l = 2$	$l = 4$	$l = 6$
-0.2341	-0.1539		
-1.678	-1.520	-1.161	-0.6244
-5.434	-5.200	-4.659	-3.826
-12.61	-12.30	-11.58	-10.46
-24.30	-23.91	-23.01	-21.61

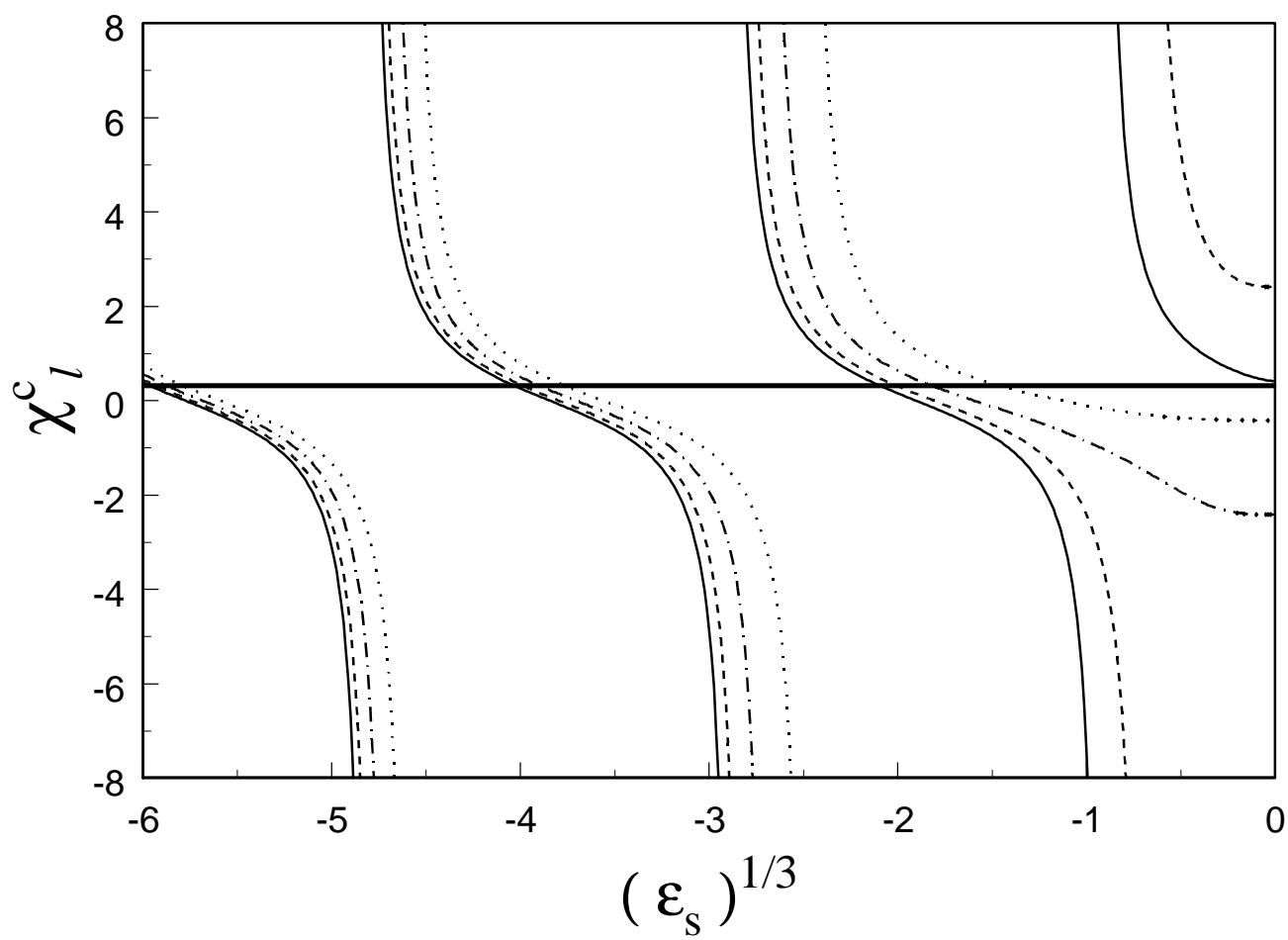


Figure 1

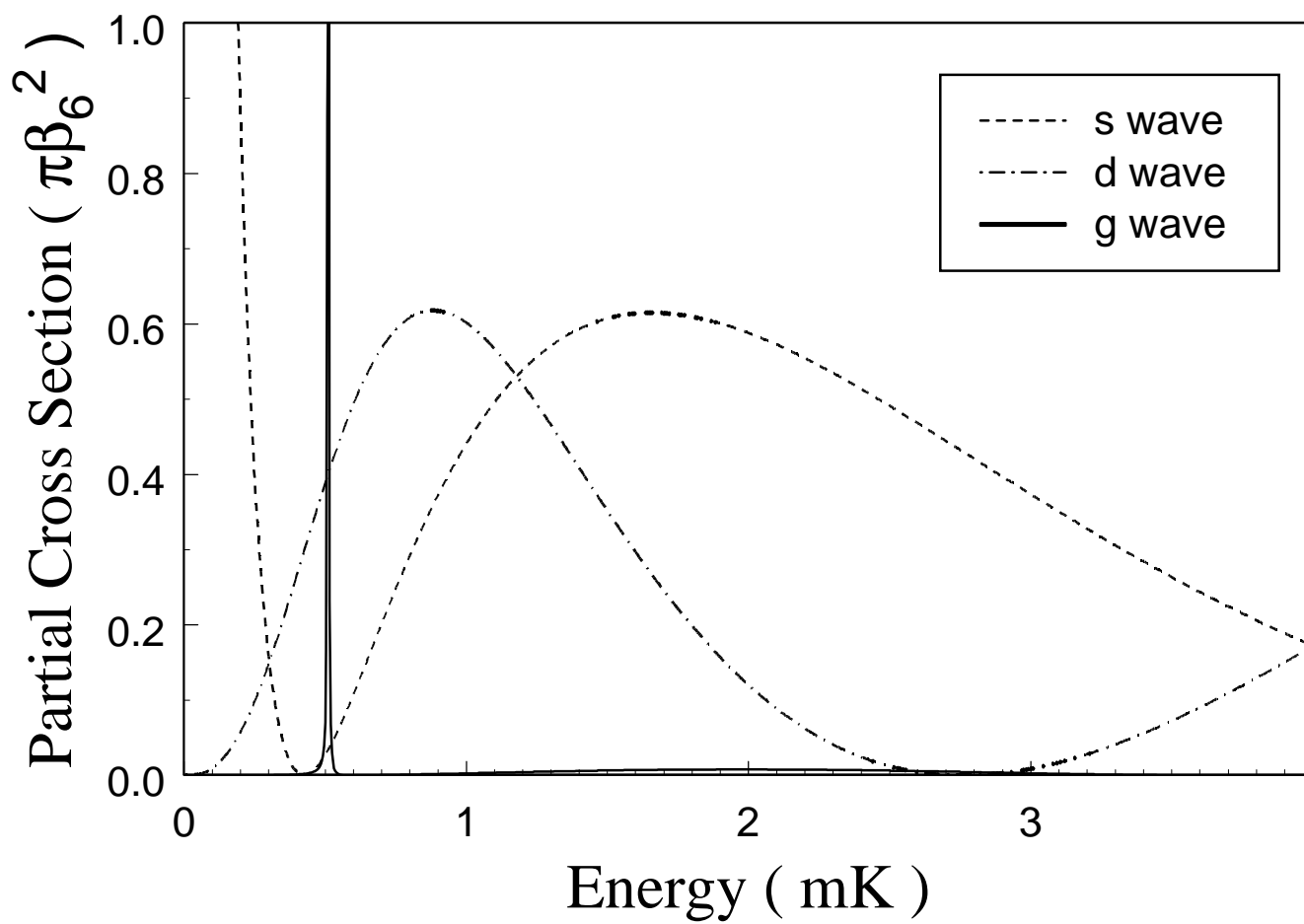


Figure 2